The Plant Cell, Vol. 8, 15–30, January 1996

Conserved Expression of the Arabidopsis *ACT1* and *ACT3* Actin Subclass in Organ Primordia and Mature Pollen

Yong-Qiang An,[a] Shurong Huang,[b] John M. McDowell,[c] Elizabeth C. McKinney,[a] and Richard B. Meagher[a,1]

[a] Department of Genetics, University of Georgia, Athens, Georgia 30602-7223
[b] Lawrence Berkeley Laboratory, University of California–Berkeley, Berkeley, California 94720
[c] Department of Biology, University of North Carolina, Chapel Hill, North Carolina 27599

We have proposed that ancient and divergent classes of plant actin genes have been preserved throughout vascular plant evolution, because they have distinct patterns of gene regulation. The hypothesis was explored for *ACT1* and *ACT3*, which represent one of the six ancient subclasses in the Arabidopsis actin gene family. Comparison of *ACT1* and *ACT3* cDNA and genomic sequences revealed highly divergent flanking and intron sequences, whereas they encoded nearly identical proteins. Quantification of their level of divergence suggests that they have not shared a common ancestor for 30 to 60 million years. Gene-specific RNA gel blot hybridization and reverse transcriptase–polymerase chain reaction analyses demonstrated that the distribution of *ACT1* and *ACT3* mRNAs was very similar: both preferentially accumulated at high levels in mature pollen and at very low levels in the other major organs. The 5′ flanking regions of both genes, including the promoter, leader exon and intron, and the first 19 codons, were fused to the β-glucuronidase (*GUS*) reporter gene. The expression of these reporter fusions was examined in a large number of transgenic Arabidopsis plants. Histochemical assays demonstrated that both *ACT1-GUS* and *ACT3-GUS* constructs were expressed preferentially in pollen, pollen tubes, and in all organ primordia, including those in roots, shoots, and the inflorescence. Comparison of the 5′ flanking regions of *ACT1* and *ACT3* revealed a number of short conserved sequences, which may direct their common transcriptional and post-transcriptional regulation. The expression patterns observed were distinct from those of any other Arabidopsis actin subclass. The conservation of their expression pattern and amino acid sequences suggests that this actin subclass plays a distinct and required role in the plant cytoskeleton.

INTRODUCTION

Actin is a fundamental component of the cytoskeleton in all eukaryotes and directs the spatial organization of many crucial subcellular processes. The presence of diverse microfilament configurations has been established in a majority of plant cell types (Parthasarathy et al., 1985; Lloyd, 1991; Meagher and Williamson, 1994). The localization of microfilaments and some physiologic studies suggest that distinct microfilament arrays govern important processes, including determination of division plane during cytokinesis, cell elongation, and cell wall deposition, which are critical to plant development and cell differentiation (Kobayashi et al., 1987; Lloyd, 1991; Cleary et al., 1992). The response of plants to external stimuli, such as the gravitrophism of root growth and light on chloroplast streaming and orientation, may also require the actin-based cytoskeleton (White and Sack, 1990; Ytow et al., 1992). The molecular genetic bases for the complex temporal and spatial regulation of these cytoskeletal processes (Staiger and Schliwa, 1987) are not well understood.

Actin is encoded by gene families in most multicellular eukaryotes. In soybean, the actin gene family encodes at least three subclasses of actin, which are more divergent from one another than vertebrate cytoplasmic actin is from muscle actin (Hightower and Meagher, 1986). Similar observations have been reported in several other plant species (Baird and Meagher, 1987; Drouin and Dover, 1990; McElroy et al., 1990a; Thangavelu et al., 1993). Quantitative evolutionary studies suggest that the different actin subclasses diverged very early in vascular plant evolution, perhaps 300 to 500 million years ago (Hightower and Meagher, 1986). It has been proposed that such ancient and divergent gene family members have been maintained in the plant genome because they have distinct patterns of regulation and/or encode proteins with distinct functions.

Recent studies have shown that plant actin genes are expressed differentially (Meagher and Williamson, 1994). Three subclasses of soybean actin genes show >100-fold variation in the levels of RNA expressed in various organs. The expression of the μ-actin subclass is regulated positively by light and auxin (Hightower and Meagher, 1985). In situ immunolocali-

[1] To whom correspondence should be addressed.

zation has demonstrated that the λ subclass of actins is expressed strongly and preferentially in root protoderm (McLean et al., 1990), whereas the κ subclass of actins accumulates in all root tissues except root cap. Two rice actin genes also exhibit differential RNA expression during early seedling development (McElroy et al., 1990a). One rice actin gene, *RAc1*, is constitutively expressed in many tissues in transgenic plants (Zhang et al., 1991). *TAc25*, a tobacco actin gene, was preferentially expressed in mature pollen (Thangavelu et al., 1993). These initial data suggest a diversity of plant actin expression patterns to match the diversity in plant actins.

We hope to understand the forces that have preserved the ancient plant actin gene family and the functions of each actin gene member. This requires a comprehensive characterization of all actin gene family members in one organism and a detailed examination of the expression pattern of each family member at the tissue level. Arabidopsis appears to be an excellent organism for this undertaking, because it has a relatively simple actin gene family (McDowell et al., 1996) and a small genome that affords a comprehensive characterization (Meyerowitz, 1989). The 10 Arabidopsis actin genes that have been isolated and sequenced in our laboratory, including the two presented herein, probably represent the entire actin gene family (McDowell et al., 1996). Based on the level of replacement nucleotide substitution (RNS), the genes are divided into six subclasses, which show the level of divergence observed previously among plant actin family members. Any two subclasses differ by 3 to 9% RNS and are thought to be >200 million years diverged from a common ancestral sequence (McDowell et al., 1996).

In this study, we present the isolation and characterization of one Arabidopsis actin subclass, that encoding *ACT1* and *ACT3*, and we explore the hypothesis that the diverse actin gene subclasses are regulated differentially. These two actins are only ~30 to 60 million years diverged from a common ancestral actin gene (McDowell et al., 1996). Their detailed tissue-specific expression patterns are examined at various developmental stages. *ACT1* (Nairn et al., 1988) and *ACT3* encode nearly identical proteins, with only one conservative amino acid difference, and yet their level of nucleotide divergence is very high in silent nucleotide sites within codons, in noncoding flanking regions, and in introns. Both genes were expressed preferentially in mature pollen and pollen tubes and in all organ primordia examined.

RESULTS

Isolation and Characterization of *ACT1* and *ACT3*

Two different Arabidopsis genomic libraries were screened with either Dictyostelium actin cDNA or soybean actin genomic DNA fragments as probes. Ninety-one recombinant phages that hybridized to either probe were randomly selected from the positive clones and subjected to partial characterization. Of the 91 clones, six were defined as *ACT1* and 12 as *ACT3*. Complete sequence analysis revealed that *ACT1* and *ACT3* each encoded 377-amino acid actin proteins that were nearly identical (see Discussion), and these were placed into a separate

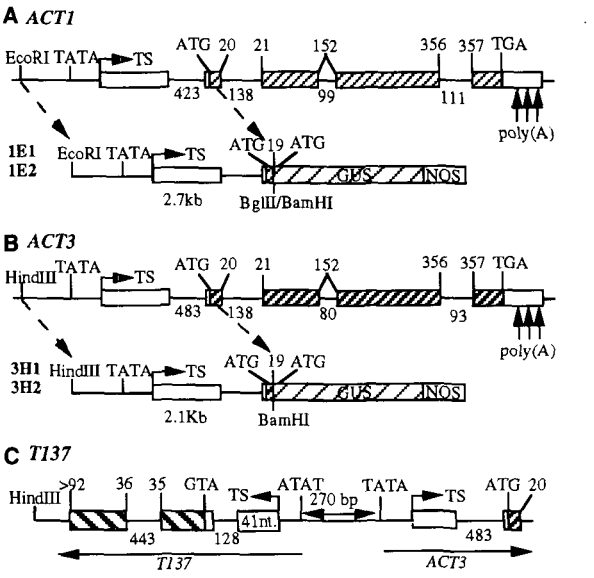

Figure 1. Gene Structures and *GUS* Fusion for *ACT1* and *ACT3*, and the Close Linkage between *T137* and *ACT3*.

(A) and **(B)** The physical structures of *ACT1* (top) and *ACT3* (top) were characterized in detail. Both *ACT1* and *ACT3* encode 377-amino acid proteins. The translated portions of exons are denoted by heavily striped boxes, untranslated portions of the mature transcripts by open boxes, and introns and nontranscribed flanking regions by lines. The lengths of the introns in base pairs are indicated. The number at the boundaries of each exon indicates the codon(s) at which the intron is located. Intron 2 splits glycine codon 152 in phase 2. The positions of the translational initiation site (ATG) and stop codon are also indicated. Both *ACT1* and *ACT3* have multiple transcriptional start sites and polyadenylation sites. The 5′ flanking regions of *ACT1* (bottom) and *ACT3* (bottom), including the promoter region, exon L, intron L, and the first 19 codons, were fused in frame to the *GUS* reporter gene (boxes labeled GUS) at the BamHI site of the pBI101.1 binary expression vector. The 3′ region of the nopaline synthase gene (open boxes) provided 3′ RNA processing and polyadenylation signals. The lengths of the 5′ flanking regions and cloning sites used for fusion constructs are indicated.

(C) The partial structure of the *T137* gene and its proximity to the *ACT3* gene are shown. A partial sequence of the cDNA, *T137*, was found ~300 bp upstream from *ACT3*. *T137* and *ACT3* are transcribed in opposite directions (indicated by long arrows), and their TATA boxes (ATAT for *T137*) are only 270 bp apart (the two-headed arrow). The unique transcriptional start site mapped for *T137* is indicated with the arrow labeled (TS). Based on the available *T137* cDNA sequence, its coding region (heavily striped box) and 5′ UTR (open box) are indicated. The putative translational start codon (ATG) is marked by GTA, because the *T137* gene is shown in reverse orientation. nt, nucleotide.

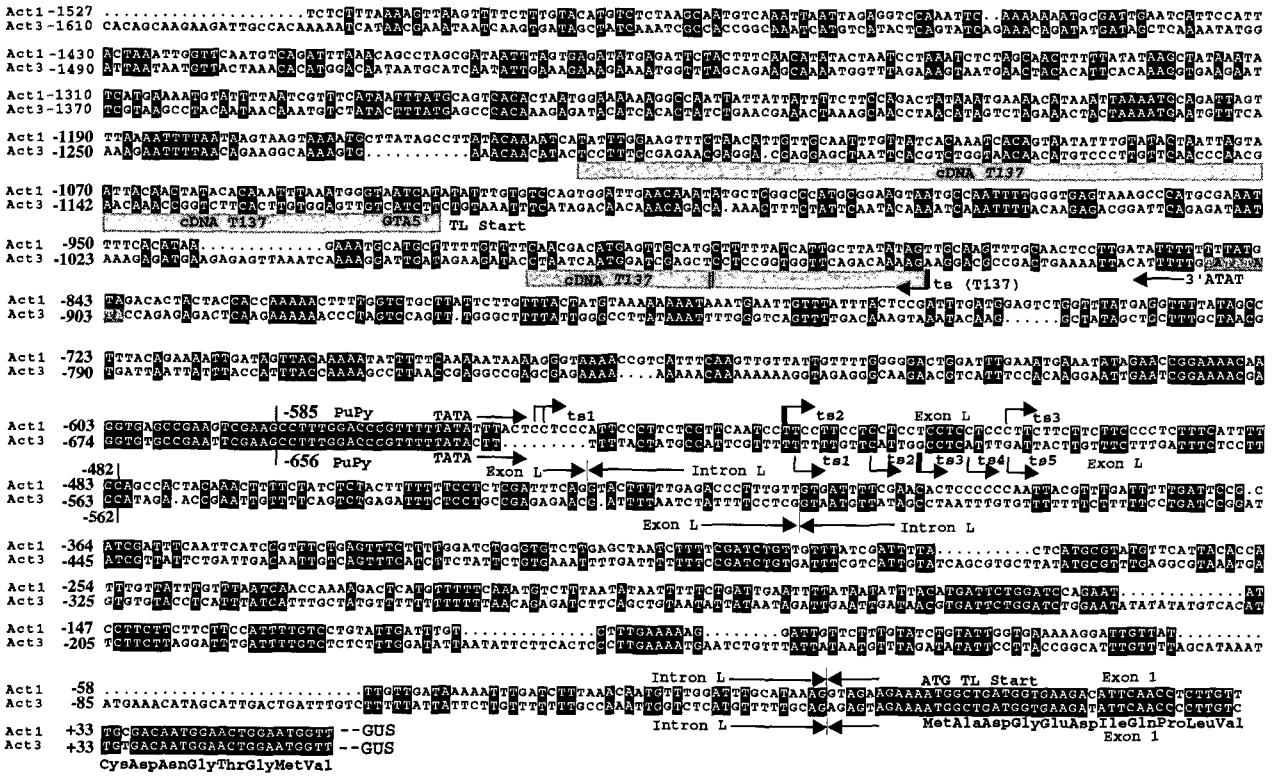

Figure 2. Alignment of the *ACT1* and *ACT3* 5′ Flanking Sequences Reveals Conserved Elements.

Approximately 1.6 kb of 5′ flanking sequences, including the first 19 codons of *ACT1*, were aligned with the corresponding sequence of *ACT3*. The nucleotides are numbered from the translational initiation site (the A of ATG initiator is +1). Identical nucleotides shared by both sequences are highlighted with a black background. The first 19 amino acids of *ACT1* and *ACT3* are also identical and are shown under the corresponding nucleotide sequences. The putative TATA boxes, the transcriptional start sites, the 5′ and 3′ splicing sites of intron L (lines with arrows), and the start codon are indicated. The boundaries of the pyrimidine-rich regions are marked by vertical lines and are numbered. The cDNA, *T137*, was located upstream and transcribed in the opposite direction from *ACT3*. The sequences complementary to the *T137* cDNA are underlined by gray boxes. The translational initiation site (GTA 5′), transcription start sites (lines with arrows), and TATA box (3′ ATAT) of *T137* are marked. *ACT1* and *ACT3* have GenBank accession numbers U39449 and U39480, respectively.

actin subclass (McDowell et al., 1996). *ACT1* was identical to the only previously identified Arabidopsis actin gene sequence, which has been partially sequenced (Nairn et al., 1988). Figures 1A and 1B show the complete gene structures of *ACT1* and *ACT3*. Based on comparison with known plant actin sequences, three introns were identified in each coding sequence; all were <138 bp. They were positioned between codons 20 and 21, within codon 152, and between codons 356 and 357. These locations are identical to those in most characterized plant actin genes (Meagher and Williamson, 1994). A few well-characterized plant actin genes have been shown to contain a large intron in the 5′ untranslated region (5′ UTR) of the mRNA (McElroy et al., 1990b; Pearson and Meagher, 1990). To determine whether *ACT1* and *ACT3* have an intron in this position, the 5′ UTRs of their cDNAs were amplified from a flower cDNA library by a polymerase chain reaction (PCR) protocol (see details in Methods). Comparison of the sequences of the PCR products with the genomic sequences revealed that both *ACT1* and *ACT3* had relatively large introns (423 and 483 bp, respectively) 10 nucleotides upstream from the ATG initiation codon.

Primer extension analysis of RNA from pollen indicated that *ACT1* transcription started at three sites spaced ~25 bp apart (Figure 2). The strongest extension product was located at 110 nucleotides (ts2) from the translation starting site of the transcript. A putative TATA box was found 32 nucleotides upstream of this start site. The two weak primer extension products, ts1 and ts3, located the 5′ ends of transcripts at 135 and 87 nucleotides, respectively, upstream of the translational start site. To confirm that the weaker upstream site was in fact used, we performed a reverse transcriptase–PCR (RT-PCR) analysis of the ts1 product. A sense oligonucleotide, ACT1-5′S1, homologous to the proposed RNA sequence between the ts1 and ts2

sites, and an antisense oligonucleotide in the first coding exon were used successfully as primers in a PCR assay to amplify this sequence from a floral cDNA library (data not shown). This result suggested that some transcription was initiated upstream of the ts2 site. Ribonuclease protection assays of the *ACT3* mRNA mapped a cluster of 5′ ends ~115 nucleotides from the translational initiation codon as shown in Figure 2. The strongest potential start site was located at 115 nucleotides (ts3), whereas four other weaker products placed sites at 128 (ts1), 120 (ts2), 110 (ts4), and 106 (ts5) nucleotides. The TATA box, located 37 nucleotides upstream of this site, is apparently conserved between *ACT1* and *ACT3*. Multiple start sites have been found in many of the plant actin transcripts that have been examined in detail (Pearson and Meagher, 1990).

Although *ACT1* and *ACT3* encoded nearly identical proteins with one conservative amino acid difference (see Discussion), the nucleotide sequences of the introns (data not shown) and 5′ (Figure 2) and 3′ (data not shown) flanking regions were highly divergent. However, the 5′ flanking sequence also contained a few conserved sequence blocks. Most obvious was a 55-bp contiguous sequence with 50 bp of identity, which included the putative TATA box. Eleven more sequence blocks with more than six nucleotides of identity were found in the 1.5-kb 5′ flanking sequence. Several short insertions or deletions were also found in the 5′ flanking region. In addition, each gene had a pyrimidine-rich stretch located in the leader exon and the adjacent region of its promoter. Within a 108-nucleotide sequence in *ACT1*, 96 nucleotides were pyrimidines, whereas 75 of 98 nucleotides were pyrimidines in the corresponding region of *ACT3*. In addition, CCT, CCTT, and TTC repeats dominated the *ACT1* pyrimidine-rich region.

To define precisely the polyadenylation sites of *ACT1* and *ACT3*, 3′ cDNA fragments of *ACT1* and *ACT3* were amplified by a modified 3′ rapid amplification of cDNA ends (RACE-PCR) procedure (see Methods) from a flower cDNA library and cloned into pBluescript II SK+ vector. The 3′ ends of a number of independent *ACT1* and *ACT3* cDNA clones were sequenced. Four polyadenylation sites were found in seven independent *ACT1* clones. They were located 205, 208, 229, and 315 bp downstream of the stop codon. Polyadenylation at position 208 was found in four clones and, thus, it might be a preferential site for polyadenylation or an artifact of PCR amplification and cloning. Three polyadenylation sites were found among three clones of *ACT3*, and they were located 246, 270, and 273 bp downstream of the stop codon (3′ sequences are not shown).

To investigate whether other genes are closely related to *ACT1* and *ACT3*, 5′ flanking sequences from *ACT1* and *ACT3* (2.7 and 2.1 kb, respectively) were used as gene-specific probes for Arabidopsis genomic DNA. Figures 3A and 3B show the hybridization results. Among the five different restriction enzyme digestions (EcoRI, HindIII, BglII, XbaI, and HincII), all produced a single hybridizing band, except the lane containing XbaI for *ACT3*. From the available sequence, XbaI digestion cleaves 1.2 kb upstream of the *ACT3* start codon, resulting in two fragments that hybridize to the probe. These and similar experiments with probes derived from the 3′ UTRs (McDowell et al., 1996) strongly suggest that *ACT1* and *ACT3* are encoded by single genes in Arabidopsis.

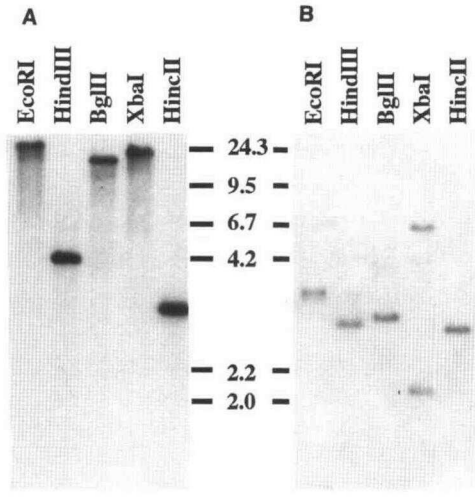

Figure 3. Genomic DNA Gel Blot Analysis.

ACT1 and *ACT3* are each unique sequences in the Arabidopsis genome.
(A) Five micrograms of genomic DNA restricted with EcoRI, HindIII, BglII, XbaI, or HincII and resolved on a 0.8% agarose gel was blotted to a nylon membrane and hybridized with a ^{32}P-labeled *ACT1* 5′ region gene–specific probe.
(B) A parallel set of restriction endonuclease–digested genomic DNA on a nylon membrane hybridized with the *ACT3* 5′ region gene–specific probe. Positions of the molecular length markers in kilobases are shown between the two autoradiograms. Hybridization conditions are described in Methods.

Preferential Accumulation of *ACT1* and *ACT3* mRNA in Mature Pollen

RNA gel blot hybridization was used to investigate the distribution of *ACT1* and *ACT3* mRNAs in various organs. The 3′ untranslated regions (3′ UTRs) of *ACT1* and *ACT3* were highly divergent from each other and from the other Arabidopsis actin genes and were used as gene-specific probes for RNA gel blot analysis. The 3′ UTRs of *ACT1* and *ACT3* did not show cross-hybridization with any other Arabidopsis actin genomic DNA, as shown at the bottom of Figures 4A and 4B. Total RNA was isolated from roots, stems, leaves, flowers, pollen, and siliques and loaded in each lane in equal amounts. Both *ACT1* and *ACT3* mRNAs were accumulated preferentially in the pollen and are ~1.6 kilonucleotides in length (Figure 4, top). The levels of *ACT1* RNA were extremely high in pollen, whereas only weak hybridization signals were detected in the stems and flowers. No visible signals were detected in roots, leaves, or siliques after

a 3-day exposure of the autoradiogram. The ratio of pollen expression to that in stems or flowers was higher for *ACT1* mRNA than for *ACT3* mRNA. Rehybridization of these blots with a probe for 18S ribosomal RNA confirmed that equal amounts of total RNA were resolved in each lane of the agarose gel and were transferred to the filters (Figure 4).

Gene-specific RT-PCR was used to verify the levels of *ACT1* and *ACT3* mRNA observed by RNA gel blot analysis. After normalizing for small variation in the levels of cDNA synthesis, the cDNA samples from leaves, pollen, roots, stems, flowers, and siliques were assayed as a twofold dilution series. The primers spanned intron 3 to detect possible genomic DNA contamination in the RNA, because the genomic PCR products would be larger (see Methods). Figure 5A shows the RT-PCR results for *ACT1*. The expected sizes of the cDNA products were obtained, and no genomic DNA contamination was detected in any sample. The levels of *ACT1* RT-PCR products from various organs agreed with the results from RNA gel blot analysis. *ACT1* products were extremely high in pollen, but only weak

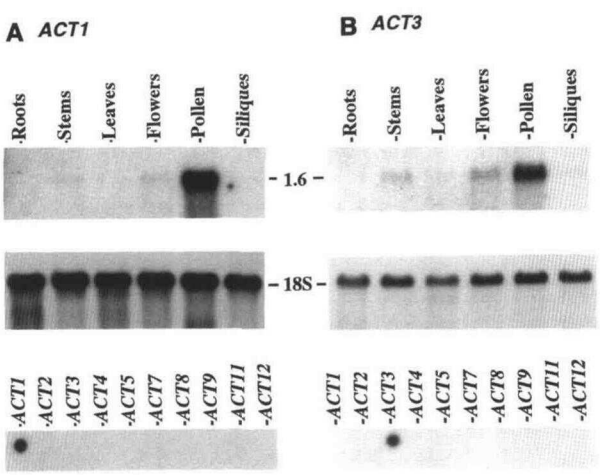

Figure 4. RNA Gel Blot Analysis of *ACT1* and *ACT3* Transcript Levels in Major Plant Organs.

ACT1 and *ACT3* transcripts were most highly expressed in pollen.
(A) Five micrograms of total RNA from roots, stems, leaves, flowers, pollen, and siliques was resolved on 1.0% agarose–formaldehyde gels, blotted onto nylon membranes, and hybridized with a ^{32}P-labeled gene-specific probe from the 3′ UTR of *ACT1*. The autoradiogram is shown (top). To confirm equal loading of RNA, membranes were stripped and reprobed with a ^{32}P-labeled oligonucleotide complementary to the 18S rRNA, RRNA1637 (Table 1), and exposed for 30 min (middle). The positions of the hybridizing actin transcripts (top; 1.6 kilonucleotides) and the 18S rRNA (middle) are indicated.
(B) Autoradiogram of an identically prepared filter hybridized with the *ACT3* 5′ UTR (top) and reprobed with an 18S rRNA probe (middle; 10-min exposure). At the bottom of **(A)** and **(B)**, the gene specificity of the *ACT1* and *ACT3* 3′ UTR probes is demonstrated by hybridization to the plasmid subcloned DNAs from each of the 10 different Arabidopsis actin genes.

product bands were seen from the leaves, roots, stems, and the floral organ complex. Based on the RT-PCR assay, the *ACT1* mRNA was at least 128 times more abundant in mature pollen than in stems and flowers. The distribution of *ACT3* mRNA from RT-PCR analysis, shown in Figure 5B, also was consistent with the results from RNA gel blot analysis. *ACT3* RT-PCR products preferentially accumulated in the pollen but were only approximately four to eight times higher in pollen than in leaves, stems, or flowers.

Expression of *ACT1* and *ACT3* Reporter Fusions in Transgenic Arabidopsis Plants

To determine precisely the expression patterns of *ACT1* and *ACT3* with respect to specific tissues and developmental stages, 2.7 kb from *ACT1* and 2.1 kb from *ACT3* 5′ flanking regions were coupled to the bacterial β-glucuronidase (*GUS*) coding sequence in a translational fusion. The 5′ flanking region of each actin gene included its putative promoter (~2.0 kb for *ACT1* and ~1.5 kb for *ACT3*), leader intron (423 bp for *ACT1* and 483 bp for *ACT3*), 5′ UTR, and 19 N-terminal codons of actin. The *ACT1–GUS* and *ACT3–GUS* fusion constructs are shown in Figure 1, and the histochemical data are summarized in Figures 6A to 6M.

Five to 10 independent transgenic plant lines for each construct were regenerated (T_0 generation), and T_1 or T_2 plants from each independent transgenic plant line were examined with histochemical assays for *GUS* expression. Some variations were observed in the intensity of GUS activity within and among independent transgenic plant lines. However, no significant variation was seen in the pattern of GUS activity except as noted. The expression patterns of the two independent constructs for each actin gene (1E1 and 1E2, and 3H1 and 3H2) showed no significant difference, demonstrating that no important sequence element was mutated in making the constructs. Nontransformed plants showed no GUS activity in any tissue after a 3-day incubation under the assay conditions used.

Preferential Expression of *ACT1-GUS* in Root Tips and Shoot Apex of Vegetative Tissues

The distribution of GUS activity from the *ACT1–GUS* construct was examined in the vegetative organs of 3- to 7-day-old seedlings (Figure 6A) and juvenile plants (Figure 6B). In seedlings, strong GUS activity was consistently observed in the root tips and shoot apex, including the apical meristem of seedlings, which turned dark blue after only 1 to 5 hr of staining with the GUS substrate (Figures 6A, 6D, and 6G). The strong staining in root tips was restricted primarily to the root cap and meristematic region (Figure 6G). Strong GUS activity was also observed in the first lateral root primordia, which forms in the transition zone (Figure 6F). Low levels of GUS activity were often observed in vascular tissues of the cotyledon, the

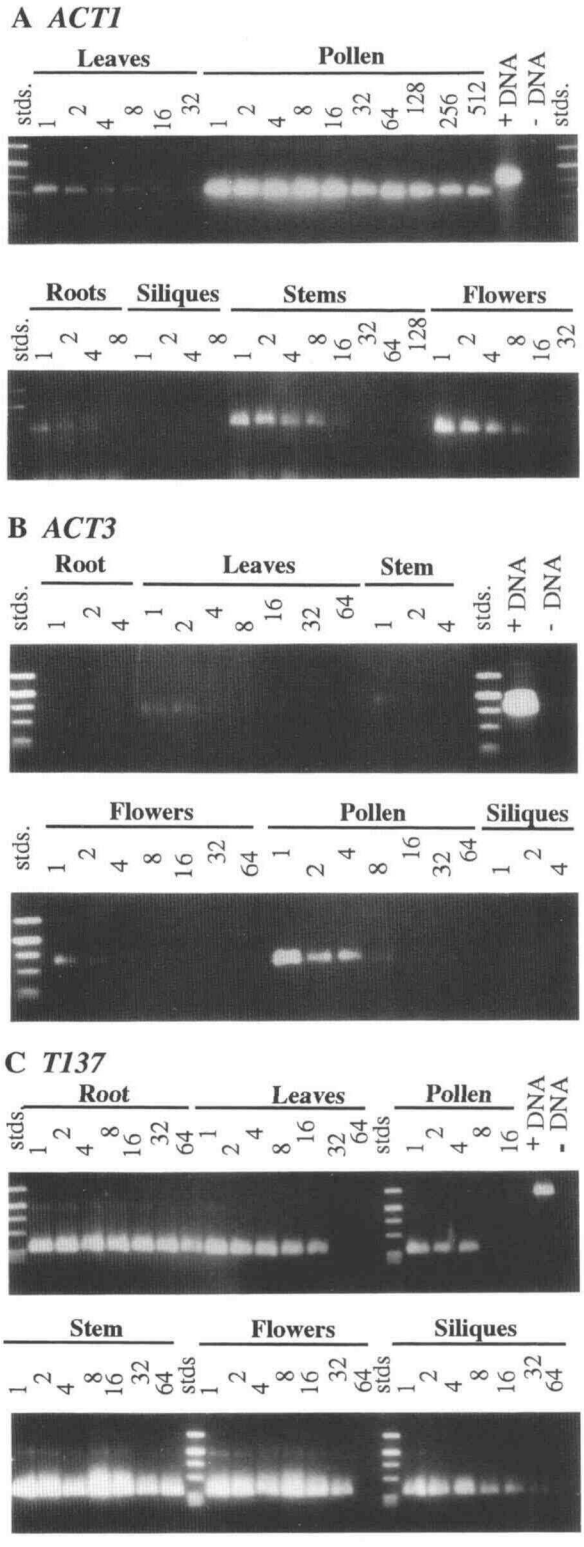

Figure 5. RT-PCR Analysis of *ACT1*, *ACT3*, and *T137* Transcript Levels in Major Plant Organs and Pollen.

hypocotyl, and the youngest portions of the root, whereas the other tissues of the seedling showed no or little GUS activity (Figure 6A). The variability in young vascular tissue expression can be seen by comparing Figures 6A, 6D, and 6F.

In juvenile plants ~3 weeks old, the root system showed essentially the same expression pattern as in seedlings (Figure 6B). GUS activity continued at the highest levels in the root tips and was strong in lateral root primordia. Little or no GUS activity was observed in tissues surrounding the lateral root primordia, including the pericycle, which differentiates into the primordia. This suggests that the activation of *ACT1–GUS* transcription was concomitant with the initiation of the lateral root primordia (Figure 6H). Low to moderate levels of GUS activity were again observed in the young vascular tissue (Figure 6B).

In aerial tissues of juvenile plants, the shoot apex continued to show the higher levels of GUS activity (Figure 6E). The adjacent stipules also stained dark blue (Figure 6E). Expanding and expanded leaves showed highly variable levels of GUS activity. The staining in expanded leaves from different transgenic plants ranged from no GUS activity to moderate levels of GUS activity. The younger leaves consistently showed much higher levels of GUS activity than older leaves (Figure 6B). In those plants in which *GUS* was still expressed in fully expanded leaves, the activity was located preferentially in the vascular tissue, hydrathodes, and trichomes.

(A) Total RNA from leaves, pollen, roots, stems, flowers, and siliques was reverse transcribed. Five nanograms of cDNA from each organ was dispensed in a twofold dilution series. For example, the first sample (1×) has 2.5 ng of input cDNA, the second (2×) has 1.25 ng, the third (4×) has 0.625 ng, the fourth (8×) has 0.312 ng, and so forth. *Each sample was then subjected to ACT1 gene–specific PCR amplification* of a 3′ portion of the gene spanning one intron in the genomic DNA. One-tenth of the product was resolved in a 1.5% agarose gel. The tissues and the level of dilution (1× to 512×) are indicated above the corresponding products. The dilution half-point (i.e., the dilution between the lowest cDNA input that produced a visible band and the cDNA input at which the reaction is still saturated) was estimated (see Methods).

(B) An identically prepared dilution series of cDNAs was subjected to *ACT3* gene–specific PCR amplification of a 3′ portion of the gene spanning one intron in the genomic DNA.

(C) An identically prepared dilution series of cDNAs was subjected to *T137* gene–specific PCR amplification of a 5′ portion of the gene spanning one intron in the genomic DNA.

The positive controls (+DNA) contain the PCR amplification products of *ACT1*, *ACT3*, and *T137* genomic DNA and indicate the position of a band expected if any cDNA sample was contaminated with genomic DNA. The negative controls (−DNA) contain the reaction products without input DNA. AluI-digested pBR322 was used as a size standard. (See details in Methods.)

Expression of *ACT1-GUS* in Floral Primordia, Mature Pollen, and Pollen Tubes

The expression of the *ACT1-GUS* constructs in the reproductive tissues was regulated in a developmental and tissue-specific manner in the inflorescence of 5- to 6-week-old plants. In Arabidopsis, the flowers and siliques can be examined easily at various developmental stages because the more mature structures are lower in the inflorescence. Figure 6C shows the staining of one *ACT1-GUS* inflorescence. Strong GUS staining was first observed in the floral primordia and young flower buds (Figures 6C and 6J). As the flowers matured, GUS activity became restricted to the young developing gynoecium, where subsequently it dropped off to undetectable levels (Figure 6C). When flowers were close to anthesis, the pollen sack of the anthers stained dark blue (Figure 6I). Strong staining in the anther was usually restricted to pollen, although weak activity was observed occasionally in the anther sac (Figure 6K). Staining of chromosomes with 4′,6-diamidino-2-phenylindole indicated that *GUS* expression was first observed in trinucleate pollen (data not shown). In vitro–germinated pollen tubes (Figure 6L) or pollen tubes on a native stigma (Figure 6M) showed high levels of GUS activity in the vegetative cell. Because sperm cells are embedded in the blue cytoplasm of vegetative cell, we were not able to determine whether *GUS* was expressed in sperm cells, in which F-actin is yet to be reported (Palevitz and Liu, 1992). In opened flowers, there was little or no GUS activity in sepals, petals, stalks, filament, or pistil (Figure 6I). In the gynoecium, *GUS* was expressed at the micropylar end of the embryo sac within the ovule (data not shown). Low to moderate levels of GUS activity were often observed in transmitting tissues in gynoecium, floral stalks, and receptacles, presumably from penetrating pollen tubes.

ACT3-GUS Has an Expression Pattern Similar to That of *ACT1-GUS*

Detailed assays of the transgenic plants containing a construct with the 5′ flanking region of *ACT3* fused to *GUS* (*ACT3-GUS*) indicated that *ACT3-GUS* had an expression pattern almost identical to that of *ACT1-GUS*. In *ACT3-GUS* seedlings and juvenile and adult plants, strong staining was observed in the apical shoot meristem and root tips, root primordia, floral primordia, and meristems. Strong activity also was observed in pollen and germinated pollen tubes. Even the subtleties of *GUS* expression were conserved between *ACT1-GUS* and *ACT3-GUS*. For example, the stipules of juvenile plants had strong activity. Low to moderate levels of GUS activity were frequently seen in the vascular tissues of young organs. GUS activity was expressed preferentially in vascular tissues, hydrothods, and trichomes of expanding and expanded leaves. When parallel samples were stained for identical times, the relative levels of staining in *ACT3-GUS* plants appeared significantly higher in leaves and lower in pollen than the corresponding staining in *ACT1-GUS* plants. No attempt was made to quantify precisely the histochemical assays. These results agree well with the results from RNA gel blot analysis and RT-PCR assays of RNA steady state levels.

A Divergent Transcription Unit, *T137*, Lies Just Upstream of *ACT3*

Using the 5′ flanking sequence of *ACT3* to search GenBank for homologous sequences, we found that 336 nucleotides of *ACT3* were identical to the 5′ portion of a cDNA, accession number T13794 (abbreviated herein as *T137*; Figures 1C and 2). *T137* was isolated originally from a cDNA library made from a mixture of various tissues (Arabidopsis ecotype Columbia) and partially sequenced as an expressed sequence tag. The identity between *T137* and *ACT3* sequence began 349 bp upstream from the first *ACT3* transcriptional start site. The *T137* transcription unit was in the antisense orientation relative to *ACT3*. Using primer extension (see Methods), we mapped the transcriptional start site to 45 nucleotides upstream of the putative translation initiation site for the T137 protein and 29 nucleotides downstream from a putative TATA box (TATATAT). This placed the proposed TATA boxes of *T137* and *ACT3* only 270 bp apart and demonstrated that the two genes are transcribed in opposite directions. A large open reading frame was identified in the *T137* cDNA. Comparison of the *T137* sequence, the sequence of an RT-PCR product isolated for this region from a leaf cDNA library (see paragraph below), and the *ACT3* 5′ flanking sequence revealed that the *T137* coding sequence was interrupted by intervening sequences. The first intron was located three nucleotides upstream of the translational start site of the open reading frame and was flanked by the universal intron splicing sequences GT and AG. The second intron began at the putative codon 35 and extended beyond the region shown in Figure 2. A different Arabidopsis cDNA and three rice cDNAs in the sequence data base showed >68% homology with *T137*. None of these sequences showed strong similarity with any sequence of known function, and thus the functional role for *T137* is not known. The proximity of *ACT3* and *T137* suggests that they might share some regulatory elements.

Using a *T137* sense oligonucleotide (ACT3-5′N6) within the leader of *T137* identified by our primer extension data and the antisense *T137* oligonucleotide (ACT3-5′S3) located in the far upstream region of *ACT3*, we amplified *T137* cDNA from oligo(dT)-primed leaf cDNA, using PCR. The reaction produced an ~300-bp fragment, as predicted from the cDNA sequence. This result further established that *T137* is transcribed from the upstream sequence of *ACT3* and was not attached to *ACT3* due to a cloning artifact. Partial Sau3A restriction endonuclease digestions of genomic DNA were used to construct the genomic library from which the characterized *ACT3* clone was isolated. No Sau3A sites were found in the region between the two genes, excluding the possibility that the close linkage is from

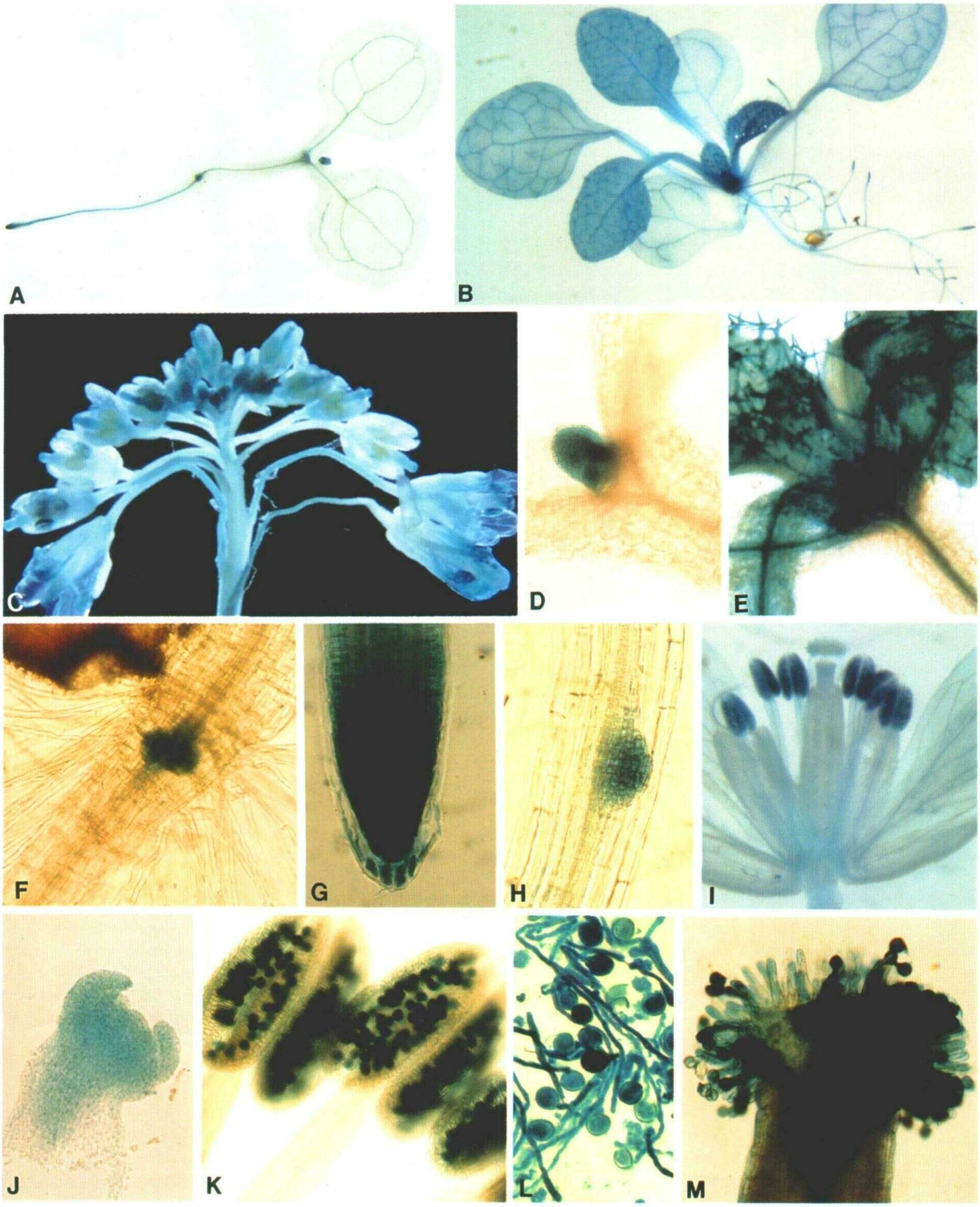

Figure 6. *ACT1–GUS* and *ACT3–GUS* Fusions Are Highly Expressed in Organ Primordia and Mature Pollen.

The expression of translational fusions of the *ACT1* and *ACT3* 5′ regions (Figure 1) with the *GUS* reporter gene was examined in transgenic Arabidopsis plants. *ACT1–GUS* expression in plants and organs as visualized by histochemical staining is shown.

two separated Sau3A fragments that were ligated during library construction. The genomic clone we isolated containing *T137* and *ACT3* was the same size as the fragment observed on gel blotting of genomic DNA (data not shown).

RT-PCR showed that *T137* RNA accumulated to a high level in all examined organs, including roots, stems, leaves, flowers, and siliques, but accumulated to a low level in pollen (Figure 5C). Thus, the distribution pattern of *T137* RNA was essentially the complement of *ACT3* mRNA.

DISCUSSION

ACT1 and *ACT3* Are Conserved in Structure and Regulation

Because *ACT1* and *ACT3* encode proteins with nearly identical amino acid sequences (i.e., there is only one amino acid difference between them), the two genes are defined as one of six ancient actin subclasses in Arabidopsis (McDowell et al., 1996). Like most characterized actin genes in plants (Meagher and Williamson, 1994), they both encode 377-amino acid proteins and are interrupted by four introns at conserved positions. The structural identity ends here, however. *ACT1* and *ACT3* are divergent in 56% of their silent nucleotide sites, and they show even greater divergence in their noncoding regions (e.g., see intron L shown in Figure 2). Based on the relatively rapid rate of change in silent nucleotide sites (~1% per million years) common to many eukaryotic genes (Meagher et al., 1989; Wolfe et al., 1989), it has been estimated that *ACT1* and *ACT3* have not had a common ancestor for 30 to 60 million years (McDowell et al., 1996). During this period, they could have diverged in both protein coding sequence and regulation. In fact, the only amino acid difference—Phe-345 in *ACT3* is Leu-345 in *ACT1*—is a moderately conservative interchange. Furthermore, the two genes showed nearly identical organ- and tissue-specific patterns of regulation. These factors indicate that the *ACT1* and *ACT3* gene sequences have been under strong functional constraints in Arabidopsis and its Brassicaceae ancestors.

Preferential Expression of *ACT1* and *ACT3* in Pollen and Organ Primordia

One major goal of this study was to examine the expression patterns of *ACT1* and *ACT3*. Gene-specific RNA gel blot hybridization and RT-PCR both showed that *ACT1* and *ACT3* RNAs accumulated preferentially in mature pollen, whereas only very low or undetectable levels of RNA were found elsewhere. Because different probes and primers were used for *ACT1* and *ACT3*, we could not compare the absolute levels of *ACT1* and *ACT3* RNA. However, based on the ratio of the RNA levels in various organs and in pollen, it appears that *ACT1* RNA was expressed more specifically in mature pollen than was *ACT3* RNA.

The tissue-specific and developmental transcriptional regulation of *ACT1* and *ACT3* were determined by high-resolution histochemical assays of transgenic Arabidopsis plants, which expressed actin–*GUS* reporter fusions. Because a long mRNA leader, leader intron, and the first 19 actin amino acids were also included in each construct, post-transcriptional processes also may have affected GUS activity. Both *ACT1–GUS* and *ACT3–GUS* showed two distinct expression programs. First, strong GUS activity was observed around and in organ primordia, including the shoot apex, apical root tips, lateral root primordia, and floral apex. The staining in young vascular tissues may be associated with the vascular cambium, which is often considered a secondary meristem. Second, *ACT1–GUS* and *ACT3–GUS* were highly expressed in pollen and pollen tubes. The expression of the *ACT–GUS* constructs in transgenic plants was consistent with RNA accumulation, suggesting that the 5′ flanking regions exert the primary control over *ACT1* and

Figure 6. (continued).

(A) Seven-day-old seedling.
(B) Three-week-old juvenile plant.
(C) Inflorescence.
(D) Shoot apex from a 7-day-old seedling.
(E) Stipules of a 3-week-old juvenile plant.
(F) Transition zone of a 7-day-old seedling.
(G) Root tip of a 7-day-old seedling.
(H) Lateral root primordium at the specialization zone of a 3-week-old plant.
(I) Mature flower.
(J) Floral primordium.
(K) Pollen sacs of a mature flower.
(L) In vitro–germinated pollen.
(M) Germinating pollen on a stigma.
The *ACT1–GUS* and *ACT3–GUS* expression patterns were indistinguishable by histochemical staining in identically prepared samples, except that *ACT1* expression was usually stronger in pollen than was *ACT3*.

ACT3 steady state RNA levels. The concordance of actin RNAs and GUS expression levels also suggests that there is little, if any, differential control over translational efficiency, unlike the results for the *ACT2–ACT8* subclass (Y.-Q. An, J.M. McDowell, S. Huang, E.C. McKinney, S. Chambliss, and R.B. Meagher, unpublished results).

Expression of the *ACT1* and *ACT3* fusion constructs was not absolutely limited to the mature pollen and meristematic tissues. Low to moderate levels of GUS product were often detected in leaves, the embryo sac, transmitting tissues in the gynoecium, receptacles, and floral stalks. Similar observations have been reported for other pollen-specific and meristem-specific genes (Twell et al., 1990; Medford et al., 1991; McCormick, 1993). For example, an α-tubulin gene is expressed in mature pollen and also is expressed in the tapetum, receptacle, and some vegetative tissues (Carpenter et al., 1992). Moreover, in rats, a wide range of ectopic expression of the striated muscle isoactins as well as an extended expression of the smooth muscle α-actin were reported (McHugh et al., 1991). Because regulatory systems evolve over millions of years, mutation acts on a sequence with a long previous history (Meagher, 1995), making it difficult to determine whether these patterns are of functional significance or accidents of evolution. Thus, whereas it is possible that these diverse *ACT1* and *ACT3* expression patterns represent a requirement for actin, it seems likely that some patterns of expression represent accidents of the combinatorial control of a complex promoter (Cavener, 1987; Dickinson, 1988). From an evolutionary viewpoint, present-day regulatory systems may not represent the most efficient solution but rather one solution that works, and the misexpression of gene products in tissues where they are not needed can escape "selection" so long as it is not harmful. The possible functions of the *ACT1* and *ACT3* genes and proteins in the actin cytoskeleton are discussed below.

Potential Elements Affecting *ACT1*, *ACT3*, and *T137* Regulation

A number of pollen-specific and meristem-specific genes have been characterized, and initial data suggest that their expression is regulated at the transcriptional level (Twell et al., 1990; Medford et al., 1991; Carpenter et al., 1992). The almost identical pollen- and meristem-specific expression patterns of *ACT1* and *ACT3* suggest that important regulatory elements should be preserved in their 5′ flanking regions. One 55-bp region upstream that included the putative TATA box contained 50 bp of identical sequence. Very little homology of significance was found farther upstream. A few conserved elements have been identified in other pollen-specific genes that determine levels of expression but not necessarily pollen specificity (Twell et al., 1990; Carpenter et al., 1992). We did not find significant sequence homology for these elements within *ACT1* or *ACT3*.

A relatively large intron was revealed in the 5′ UTRs of *ACT1* and *ACT3*. Large introns interrupting the mRNA leader are not common among plant genes but are found in actin genes from rice, tobacco, soybean, and vertebrates (Nakajima-Iijima et al., 1985; McElroy et al., 1990b; Pearson and Meagher, 1990; Thangavelu et al., 1993). McElroy et al. (1990b) reported that the intron in the 5′ UTR of rice actin, *RAc1*, is essential for strong expression in electroporated rice protoplasts. Recent studies in our laboratory have shown that the deletion of the corresponding intron and part of the 5′ UTR from the constitutively expressed *ACT2* Arabidopsis actin gene almost completely abolishes expression of a *GUS* fusion in transgenic plants (Y.-Q. An and R.B. Meagher, unpublished data). The leader exons of *ACT1* and *ACT3* also have a pyrimidine-rich stretch (PuPy) from the transcriptional start sites extending into the first exon, as has been observed in soybean and rice actin genes (McElroy et al., 1990b; Pearson and Meagher, 1990). The PuPy sequence may play an important regulatory role in a number of genes, including the maize *Alcohol dehydrogenase1* gene and human c-*myc* gene (Cooney et al., 1988; Lu and Ferl, 1992). The potential biological functions of the conserved sequences in the 5′ UTRs of *ACT1* and *ACT3* are under examination.

We were surprised to find a divergent transcript (*T137*) that initiated very close to and in the 5′ flanking region of *ACT3*. *T137* has a large open reading frame and appears to encode a protein; however, the function of this protein is not known. There does not appear to be a sequence similar to *T137* upstream of *ACT1*, unless its homolog is located beyond the region we have sequenced. We have not looked for *T137* homologs by gel analysis. Interestingly, the TATA boxes of *ACT3* and *T137* were separated only by 270 bp. Higher eukaryotic genes are usually separated by thousands of base pairs, even in the small genome of Arabidopsis. It has been reported that the human dihydrofolate reductase gene and a mismatched repair protein gene are organized in a divergent configuration with their transcriptional start sites separated by only 90 bp. A 165-bp fragment is sufficient to direct the accurate bidirectional transcription of both human genes (Shimada et al., 1989). RNA gel blot and RT-PCR analyses showed that the RNA expression pattern of *T137* is distinct from that of *ACT3* and perhaps even complementary. It seems quite possible that the expression of one gene impacts the other. For example, the expression of *ACT3* may repress *T137* expression in pollen by competition between the shared regulatory elements for transcription factors, as demonstrated for β- and ε-globin genes in chicken (Foley and Engel, 1992). The small space between *ACT3* and *T137* suggests that the promoter sequences required for their expression are both very compact. This view is further supported by the lack of sequence homology between the *ACT1* and *ACT3* promoter region beyond the 55-bp conserved region associated with their TATA boxes. Alternatively, some of the required promoter elements in all three genes might be located elsewhere, such as in the introns disrupting their 5′ UTRs (see above).

Cytoskeletal Functions of the ACT1 and ACT3 Proteins

The strong pollen and organ primordial expression observed for *ACT1* and *ACT3* suggests a few potential roles for these actins in pollen tube and primordial development. The nature

of pollen tube growth is different from that of most other plant cells because it is restricted to the tip region (Steer and Steer, 1989). Extensive studies indicate that actin plays an important role in pollen germination and tube growth (Steer and Steer, 1989; Steer, 1990; Mascarenhas, 1993). Throughout these stages, the actin arrays are very dynamic, changing from large spherical "storage" bodies in pollen grains to microfilament bundles oriented predominantly parallel to the growth axis in pollen tubes (Heslop-Harrison et al., 1986; Tiwari and Polito, 1988). The actin cytoskeleton is credited with "pulling" the two generative cells down through the pollen tube. A dense network of microfilaments located just behind the tube apex is thought to transport building materials to the rapidly expanding tip (Perdue and Parthasarathy, 1985; Pierson et al., 1986; Lancelle et al., 1987). Given the strength of *ACT1* and *ACT3* expression in pollen, it is likely they participate in some or all of these activities.

Among the eight highly expressed Arabidopsis actins, only *ACT1-GUS* and *ACT3-GUS* were expressed preferentially around and in the meristematic tissues. Recent studies have indicated that actin plays important roles in determining the position and formation of cell division planes. Because most plant cells do not migrate, regulating the division plane of individual cells in the meristem is central to programmed development in plants (Meagher and Williamson, 1994). The preprophase band of actin is thought to help determine the position and angle of the division plane, because later in development the phragmoplast grows out to the site previously occupied by the band. Actins may aid in the proper narrowing of the preprophase band and outgrowth of the phragmoplast to the division site (Palevitz, 1987; Mineyuki and Gunning, 1990). Thus, *ACT1* and *ACT3* also may be involved in programmed cell development.

Evolution of the *ACT1* and *ACT3* Actin Subclass

ACT1 and *ACT3* are 3 to 9% divergent in RNS from the six other expressed Arabidopsis actins and thus have not shared a common ancestor with these genes for ~150 to 450 million years (McDowell et al., 1996). Evidence that *ACT1* and *ACT3* actin belong to an ancient and conserved subclass comes also from comparisons with actins in other organisms. *ACT1* and *ACT3* are typically 12 to 17% diverged in RNS from animal and fungal actins and as much as 10% divergent from most other plant actins. However, they are only ~3% divergent from the pollen-specific tobacco actin gene, *Tac25* (Thangavelu et al., 1993; McDowell et al., 1996). Arabidopsis and tobacco are at least 100 to 110 million years diverged from a common ancestor. Thus, the conservation of RNS and pollen-specific gene expression suggests that *Tac25*, *ACT1*, and *ACT3* are orthologs, separated by the divergence of common ancestral organisms (McDowell et al., 1996). Furthermore, it suggests that both the protein sequence and the regulation of this ancient actin subclass have been subject to strong constraint throughout dicot and possibly angiosperm evolution.

The detailed expression patterns of Arabidopsis actin genes from five other subclasses also have been examined in our laboratory. The expression of *ACT1* and *ACT3* is distinct from that of any other actin subclass. The *ACT4* and *ACT12* subclass is the most similar in protein sequence to *ACT1* and *ACT3* (S. Huang, Y.-Q. An, J.M. McDowell, E.C. McKinney, and R.B. Meagher, unpublished results). This subclass is expressed preferentially in pollen but is not expressed in organ primordia. *ACT12* also is strongly expressed in the root cap and pericycle surrounding lateral root primordia (S. Huang, Y.-Q. An, J.M. McDowell, E.C. McKinney, and R.B. Meagher, unpublished results). *ACT11*, the next most divergent subclass, is expressed in pollen; in addition, it is the major actin gene expressed during inflorescence and ovule development (S. Huang, Y.-Q. An, J.M. McDowell, E.C. McKinney, and R.B. Meagher, unpublished results). The *ACT2–ACT8* subclass is the most divergent in sequence and shows an expression pattern that is the most divergent from that of *ACT1* and *ACT3*. The *ACT2–ACT8* subclass is expressed strongly and constitutively in most of the vegetative tissues both early and late in development, but it is not expressed in pollen or ovule (Y.-Q. An, J.M. McDowell, S. Huang, E.C. McKinney, S. Chambliss, and R.B. Meagher, unpublished results). *ACT7* has a pattern similar to that of *ACT8* but is restricted to young developing vegetative tissues and is only weakly expressed in pollen (J.M. McDowell, S. Huang, E.C. McKinney, Y.-Q. An, and R.B. Meagher, unpublished results). All of these subclasses are expressed at some level during early vascular tissue development. These data reveal remarkably complex genetic control of the actin cytoskeleton. Considering the relatively extreme protein sequence divergence found in this and other plant actin gene families, there may be a requirement for equally complex families of actin binding proteins (McDowell et al., 1996).

ACT1 and *ACT3* share common sequences and regulation in spite of being millions of years diverged from a common ancestor. This probably reflects conservation of their DNA and protein sequences and a requirement for pollen- and organ primordium–specific expression of these actin proteins. The expression of these two genes appears to have a strong developmental component that may be linked to the ancient evolution of microspores and organ primordia (Meagher, 1995). Future genetic studies, in particular the analysis of plant actin mutants (McKinney et al., 1995), will dissect the required components of *ACT1* and *ACT3* expression and distinguish them from accidents of evolution.

METHODS

Isolation of *ACT1* and *ACT3* Genomic Clones

Following the procedure described by McDowell et al. (1996), two *Arabidopsis thaliana* ecotype Columbia genomic libraries provided by J. Mulligan and R. Davis (Stanford University, Stanford, CA) and B. Hauge and H. Goodman (Massachusetts General Hospital, Cambridge, MA) were screened with a *Dictyostelium* actin cDNA fragment or soybean

actin genomic DNA. Randomly selected positive clones were partially sequenced with degenerate actin-specific oligonucleotides to identify the distinct actin genes (McDowell et al., 1996). The *ACT1* clones were shown to be identical in sequence to a partially sequenced *Arabidopsis actin gene* described previously (Nairn et al., 1988). Plasmid subclones of this genomic sequence were generously supplied by R. Ferl (University of Florida, Gainsville, FL) for further characterization. By following standard cloning techniques, an ~4.0-kb HindIII restriction fragment of *ACT3* genomic DNA was subcloned into pBluescript II SK+ (Stratagene) to produce pAAc3.

Sequence Determination and Analysis

ACT1 and *ACT3* genomic and cDNA clone sequencing was conducted by dideoxy chain termination methods using Sequenase (United States Biochemical Corp.) and fmol DNA sequencing (Promega) kits following the protocols provided by the manufacturers, except that several degenerate actin-specific primers were used (McDowell et al., 1996). Sequences were managed using the Genetics Computer Group (Madison, WI) sequence analysis software package (Devereaux et al., 1984) provided by the University of Georgia Biological Sequence computation facility. The DNA sequences upstream from codon 19 of *ACT1* and *ACT3* were aligned with the Genetics Computer Group's Pileup program and displayed with a Boxshade program provided by the University of Georgia Biological Sequence Computation Facility.

DNA Gel Blot Analysis

Genomic DNA was isolated from Arabidopsis ecotype Columbia as described previously by McLean et al. (1988). The DNA was digested, fractionated on 0.8% agarose gels at 40 V for 16 hr, and transferred to a nylon membrane (Biotrans Plus) in a Transvac vacuum blotter (Hoefer Inc., San Francisco, CA), according to manufacturer's instructions. The DNA was fixed to the membrane by 3 min of UV irradiation and 2 hr of baking at 80°C. The polymerase chain reaction (PCR) fragments containing the 2.7 kb of 5′ flanking sequences of the *ACT1* gene (or 2.1-kb 5′ region of *ACT3*) were labeled by the random primer method (Feinberg and Vogelstein, 1983) to a specific activity of ~0.5 × 10^9 cpm/μg. The probe was hybridized to the blot in 6 × SSC (1 × SSC is 0.15 M NaCl, 0.015 M sodium citrate), 5 × Denhardt's solution (1 × Denhardt's solution is 0.02% Ficoll, 0.02% PVP, and 0.02% BSA), 40% formamide, 0.2% SDS at 56°C for 48 hr. The blot was washed four times for 10 min at 56°C in 0.5 × SSC, 0.2% SDS, and exposed to X-Omat x-ray film (Kodak) with one intensifying screen for 48 hr at −70°C. The specificity of the 5′ probes for *ACT1* or *ACT3* was confirmed by hybridizing to dot blots containing the nine other Arabidopsis actin genes in an experiment similar to that described below for the 3′ untranslated region (UTR) probes. No cross-hybridization was observed (data not shown).

RNA Preparation and RNA Gel Blot Analysis

Seven-day-old seedlings, the roots, stems, and leaves of 3- to 4-week-old juvenile plants, and the flowers (~90% unopened) and siliques of 5- to 6-week-old plants were collected into liquid nitrogen and stored at −70°C before use. Total RNA was prepared from these tissues (Logemann et al., 1987). Pollen RNA was prepared following a previously described protocol (S. Huang, Y.-Q. An, J.M. McDowell, E.C. McKinney, and R.B. Meagher, unpublished results). RNA gel blotting was performed using a gene-specific 3′ UTR sequence probe prepared by PCR amplification. The PCR primers for the *ACT1* and *ACT3* probes were ACT1-376S and ACT1-3′N2 (Table 1) and ACT3-376S and ACT3-3′N1, respectively. Five micrograms of total RNA for each tissue was resolved in a 1% agarose–formaldehyde gel (Sambrook et al., 1989) and blotted onto a nylon membrane (0.45 μM; Millipore). The filters were prehybridized overnight in 1 × RNA hybridization mixture (Thompson et al., 1992) containing 40% formamide at 48°C. Hybridizations were performed for 24 hr using the conditions described above with ~3 × 10^6 cpm/mL each gene-specific probe labeled at ~6 × 10^8 cpm/μg of DNA by the random primer method (Feinberg and Vogelstein, 1983). Filters were washed once at 48°C for 15 min in 2 × SSC, 0.2% SDS, and two times for 15 min in 1 × SSC, 0.2% SDS. After drying briefly, the filters were exposed to X-film (Kodak) with two intensifying screens at −70°C for 1 to 3 days. Gene specificity of the probes was confirmed by hybridization to dot blots containing the nine other Arabidopsis actin genomic DNA. No cross-hybridization was observed to the incorrect clone (Figure 4). rRNA hybridization was used to monitor equal loading and transfer of the RNA samples. The RNA gel blots were stripped and rehybridized with a 26-nucleotide 18S rRNA antisense oligonucleotide, RRNA1637 (Table 1), as described previously by Tanzer and Meagher (1994). The hybridization was performed at 48°C for 20 hr with ~10^7 cpm of the probe labeled at ~10^6 cpm/pmol of oligonucleotide. Filters were washed three times, for 15 min each, at 48°C in 2 × SSC, 0.5% SDS. After brief drying, the filters were exposed to x-ray film for 10 to 30 min with two intensifying screens.

Reverse Transcriptase–PCR Analysis

Samples of total RNA (5 μg) from seedlings, roots, stems, leaves, flowers, pollen, and siliques were reverse transcribed into cDNA in 50-μL reactions with eight units of avian myoblastosis virus reverse transcriptase (Promega) and primed with 40 pmol of oligo(dT) in the manufacturer's recommended buffer. The level of cDNA synthesis was measured by assaying DNA concentration with Hoechst dye in a DNA minifluorometer (Hoefer, Inc.), following the manufacturer's instructions. The total yield typically ranged from 100 to 300 ng. An aliquot of the cDNA was dispensed in a twofold dilution series in the PCR buffer described below, such that the first sample in the series contained 2.5 ng of cDNA. The oligonucleotide primers (50 pmol of each) ACT327S and ACT1-3′N2 for *ACT1*, ACT327S and ACT3-3′N1 for *ACT3*, and ACT3-5′S3 and ACT3-5′N6 for *T137* (Table 1) were used to amplify each diluted cDNA sample. For the actin cDNAs, the amplified region included the last intron junction for the actin cDNAs and the first intron junction for the *T137* cDNA. Potential genomic DNA contamination could be ruled out based on the length of the products, because the genomic products would have been ~100 bp longer than the cDNA products. The 100-μL PCRs were subjected to 45 cycles at 94°C (1 min), 42°C (1 min), and 72°C (30 sec) in a buffer containing 0.1 mM deoxynucleotide triphosphates, 2.5 μg of linear acrylamide carrier, 50 mM KCl, 10 mM Tris-HCl, pH 8.8, 1.5 mM $MgCl_2$, and 0.1% Triton X-100 (Promega) and initiated by adding one unit of *Taq* polymerase. One-tenth of each sample was resolved on a 1.5% agarose gel and stained with ethidium bromide. In tissues in which the transcript was expressed most strongly, the highest cDNA concentrations gave approximately the same product yield (saturation). The point at which the diluted cDNA gave approximately half of that yield was designated the dilution half-point. Each dilution series was performed several times with independent RNA preparations.

Table 1. Oligonucleotides Used in PCR, Primer Extension, and *GUS* Fusion Construction

Name	Sequence	Region of Homology	Experiments
ACT1-5'S1	5'-TCCTCCCATTCCCTTCTCCTTCAAT-3'	−750 to −726 from start codon	Mapping the leader intron
ACT3-5'S1	5'-TTCATTGGCCTCATTTGATTACTTG-3'	−606 to −582 from start codon	
PLACT11N	5'-ACCATNCCNGTNCCRTTRTC-3'	Codon 13 to 19	
ACT1-5'10N	5'-TTCACCATCAGCCATTTTCTTCTAC-3'	−10 to codon 5	
ACT1-5'NP	5'-GATAGAAAAGTTTGTAGTGG-3'	−489 to −470 from start codon	Mapping the transcriptional start sites
ACT3-5'S2	5'-TCCTTTGCGAGAACGAGGACGAG-3'	+124 to +147 from TS of T137	
ACT3-5'N10	5'-*CGCGGATCCTAATACGACTCACTATAG*GATATCCGGATCAGGAA-3'	−459 to −442 from start codon	
SP6	5'-ATTTAGGTGACACTATAG-3'	pcDNAII vector	Making probe for RNA RT-PCR analysis and mapping the poly(A) addition sites
ACT1-376S	5'-*AGCTCCCGGG*CTGAGTTCAAAGTGATCATTTTTCA-3'	−1 to +21 from stop codon	
ACT1-3'N2	3'-AGC*TCCCGGGTTACATAATAATTGAAAAATTGAAG*-3'	+224 to +228 from stop codon	
ACT3-376S	5'-*AGCTCCCGGG*TTGAGCTTGAAGTTAAGTCTGCTTC-3'	−1 to +21 from stop codon	
ACT3-3'N1	5'-*AGCTCCCGGG*TATCAAATAACCTCTCTAAACTTGG-3'	+243 to +267 from stop codon	
ACT327S	5'-ATGAARATNAARGTNGTNGCNCCNCCNGA-3'	Codon 327 to 336	
ACT3-5'S3	5'-GTTCCCAACTTCCTCTTAGCAA-3'	+321 to +300 relative to TS. of T137	
ACT3-5'N6	5'-CTTCTTTTGTCTGAACCACCGGA-3'	+21 to −2 relative to TS. of T137	
RRNA1637N	5'-AGCGACGGGCGGTGTGTACAAAGGGC-3'	18S rRNA	
T7-20	5'-TAATACGACTCACTATAGGG-3'	T7 promotor	*GUS* construction
T3-17	*5'-ATTAACCCTCACTAAAG-3'*	T3 universal sequence	
PLACT12N-Ba	5'-*CGCACGGATCC*TACCATNCCNGTNCCRTTRTCRCA-3'	Codon 12 to 19	
PLACT12N-BB	5'-*CGCACDGATCD*TACCATNCCNGTNCCRTTRTCRCA-3'	Codon 12 to 19	

N represents A, G, C, T; R, A and G; W, A and T. S and N designate sense and antisense oligonucleotides relative to *ACT3*, respectively. PLACT11N, ACT327S, and PLACT12-Ba were actin-specific degenerate oligonucleotides. ACT1-5'S1, ACT1-5'10N, ACT1-5'NP, ACT1-376S, and ACT 1-3'N2 were *ACT1*-specific unique oligonucleotides. ACT3-5'S1, ACT3-5'S2, ACT3-5'N10, ACT3-376S. ACT3-3'N1, ACT 3-5'S3, and ACT3-5'N6 were specific for *ACT3*. The italic sequences were synthetic extensions with restriction sites for cloning. Oligonucleotides were synthesized at the Molecular Genetics Instrumentation Facility (University of Georgia, Athens, GA).

Mapping of Transcriptional Start Sites, Leader Introns, and Polyadenylation Sites

The precise 5' ends of *ACT1* mRNA were mapped using the primer extension method as described by Senecoff and Meagher (1993), except that 50 μg of total RNA from mature pollen was used in each reaction. The gene-specific primer ACT1-5'NP, which hybridized to the *ACT1* leader exon (Table 1) but not to *ACT3*, was used for the cDNA extension reactions. Approximately 10^6 cpm of ^{32}P-labeled primer was used in each annealing reaction. Avian myoblastosis virus reverse transcriptase (Promega) was used to perform the reactions. The 5' ends of the *ACT3* mRNA were mapped using the RNase protection assay with minor modifications (Gilman, 1989). The DNA template for in vitro transcription was made by PCR. ACT3-5'S2 and ACT3-5'N10, which hybridized to the putative promoter region and leader intron, respectively, were used as primers (Table 1). ACT3-5'N10 contained a T7 promoter sequence at its 5' end, from which antisense RNA was transcribed in vitro. Sequencing ladders and the RNA products were examined on acrylamide gels electrophoresed at 55 to 60°C to determine precisely the 5' ends of *ACT1* and *ACT3* mRNAs. Autoradiography was performed overnight with one intensifying screen at −70°C to visualize the products.

The intron within the 5' untranslated leader was mapped by using a PCR strategy. The putative location of an intron in the 5' UTR was predicted based on the scanning model for translation (Kozak, 1989) and conserved features of 5' flanking regions of plant actin genes

(Pearson and Meagher, 1990). A sense primer and an antisense primer, which were located in the putative leader exon and first coding exon, respectively, were used to PCR amplify the RNA leader intron junctions. The *ACT1* and *ACT3* products were amplified from oligo(dT)-primed floral and pollen cDNA, respectively. The primers ACT1-5'S1 and ACT1-5'10N were used for *ACT1*; ACT3-5'S1 and PLACT11N were used for *ACT3* (Table 1). Comparing the cDNA sequence of the PCR product with the genomic sequence localized the leader introns.

The 3' polyadenylation sites were mapped by a procedure modified from the protocol for 3' rapid amplification on cDNA ends (Frohman et al., 1988) and ligation-mediated PCR (Mueller and Wold, 1989). A plasmid cDNA library was prepared from mature flowers by Invitrogen (San Diego, CA). The 3' UTRs of the actin cDNAs were PCR amplified from this library as follows.

Sense oligonucleotide primers (25 nucleotides) homologous for a region of *ACT1* (or *ACT3*), including the terminal amino acid codon 376, the stop codon, and 19 nucleotides of the 3' UTR with an XmaI site and 7-bp clamp at its 5' end, ACT1-376S (or ACT3-376S), and a 25-nucleotide vector oligonucleotide, Sp6-25, were used as the PCR primers (Table 1). The Sp6-25 oligonucleotide flanks several restriction sequences on the pcDNAII vector (Invitrogen), one of which is SacI. Ten nanograms of the plasmid library cDNA was used as the template in 100-μL PCR containing 1 × PCR buffer (50 mM KCl, 1.5 mM $MgCl_2$, 10 mM Tris-HCl, pH 9.0, 0.1% Triton X-100), the four deoxynucleotide triphosphates at 0.2 mM each, 15 pmol each PCR primer, and two units of *Taq* polymerase (Promega). PCR amplifications were performed with the following program: 94°C for 2 min; 45 cycles of 94°C for 30 sec, 48°C for 30 sec, 72°C for 30 sec; 1 cycle of 94°C for 1 min, 48°C for 2 min, and 72°C for 7 min. PCR products were then digested with SacI and XmaI and cloned into the corresponding pBluescript II SK+ (Stratagene) replacement region. Positive clones were screened by PCR for actin 3' inserts of different sizes. Representative clones of different sizes were sequenced, and the polyadenylation sites were determined by the presence of a poly(A) sequence in the cDNAs in comparison with the genomic sequence.

GUS Reporter Constructs

The Arabidopsis *ACT1* actin genomic clone pAtc4, which was generously provided by R. Ferl, contains a 4.0-kb EcoRI fragment in pUC8 that includes a 2.7-kb 5' flanking sequence upstream of the translational start site (Nairn et al., 1988). A modified ligation-mediated PCR method (Y.-Q. An, J.M. McDowell, S. Huang, E.C. McKinney, S. Chambliss, and R.B. Meagher, unpublished results) was used to amplify the 2.7-kb 5' flanking region and introduce appropriate restriction sites at both ends. The primers, PLACT12N-BB (24 bases complementary to codons 12 to 19 and an 11-base sequence containing a BglII restriction site at codon 19) and T7-20 (a vector oligonucleotide), were used for the PCR amplification (Table 1). The 2.1-kb *ACT3* 5' flanking region fragment was obtained by PCR amplification of pAAc3, using T7-20 and PLACT12N-Ba as the primers (Table 1). PLACT12N-Ba is similar to PLACT12N-BB, but it contains a BamHI site at codon 19.

A 2.7-kb HindIII-BglI–digested *ACT1* PCR product and a 2.1-kb HindIII-BamHI–digested *ACT3* PCR product were ligated with HindIII-BamHI–digested pBI101.1 (Jefferson et al., 1987) to produce the actin β-glucuronidase (*GUS*) translational fusion constructs *ACT1–GUS* and *ACT3–GUS*. A total of 27 codons, including eight codons created from the vector sequence, were added to the N terminus of the wild-type *GUS* sequence. The 3' region of nopaline synthase gene was used in this vector to direct polyadenylation (Jefferson et al., 1987). Two constructs, each from an independent PCR (1E1 and 1E2 from the *ACT1* 5' region; 3H1 and 3H2 from the *ACT3* 5' region) were made for each gene to control for potential PCR-generated mutations in regulatory elements. The expression patterns of all constructs were compared with the control for effects of possible PCR-generated mutations and to increase the total number of transgenic plants examined. Approximately 500 bp of sequence upstream from the fusion sites were examined, and 0- to 2-bp changes from the parent sequence were found in each; however, none of these changes produced reading frame shifts or occurred in any conserved elements (see Results and Discussion). The constructs were mobilized into *Agrobacterium tumefaciens* LBA4404 after a direct transformation protocol (An et al., 1988).

Plant Transformation and Growth

T-DNAs carrying the *ACT1–GUS* and *ACT3–GUS* constructs were transformed into Arabidopsis embryos, and T_0 plants were regenerated as described previously by Marton and Browse (1991), with modifications (Y.-Q. An, J.M. McDowell, S. Huang, E.C. McKinney, S. Chambliss, and R.B. Meagher, unpublished results). T_1 transgenic seeds from the T_0 plants were germinated, and plants were grown in B5 agar-based medium plus 50 mg/L kanamycin without sucrose or vitamins under a 16-hr photoperiod at 22°C. Seedlings (3 to 7 days old) and juvenile plants (~3 weeks old) were harvested for histochemical GUS assays. After 3 to 4 weeks on plates, juvenile plants were transferred into soil for flowering. Inflorescence, flowers, and siliques were examined from 5- to 6-week-old plants. All histochemical assay data presented in this study were obtained from T_1 or T_2 plants.

Histochemical GUS Assays

Histochemical assays for GUS activity were conducted according to the protocol described previously by Jefferson et al. (1987), with some modification. Fresh tissue samples were fixed in 90% acetone on ice for 1 hr and then were washed in 50 mM $NaPO_4$, pH 7.0, twice for 30 min each (Hemerly et al., 1993). GUS staining was performed by incubating tissues in 50 mM $NaP0_4$, pH 7.0, containing 0.5% Triton X-100, 0.5 mM X-gluc (Jersey Lab Supply, Livingston, NJ), 0.5 mM $K_3[Fe(CN)_6]$, and 0.5 mM $K_4[Fe(CN)_6]$ for 1 to 24 hr at 37°C. The stained tissues were washed once with the 50 mM $NaPO_4$, pH 7.0, and bleached in several changes of 70% ethanol. The samples were examined and photographed under a Wild M5A dissecting microscope (Heerbrugg, Switzerland) and Zeiss Standard 16 compound microscope (Oberkochen, Germany) using Kodak Ektachrome 64T Professional Film.

ACKNOWLEDGMENTS

This work was supported by a basic research grant from the Molecular Cytology Study Section of the National Institutes of Health (NIH) to R.B.M. An NIH training grant to the Genetics Department at the University of Georgia supported J.M.M. Y.-Q.A. submitted portions of this work in his Ph.D. dissertation. We thank Julie Senecoff, Dima Belostotsky, and Michael Weise for their help with several technical and scientific problems and the computational analysis of sequences and Wayne Parrott and Ronald Nagao for reading drafts of the manuscript. We also thank Dr. Robert Ferl for providing his *ACT1* genomic clone.

Received July 31, 1995; accepted November 2, 1995.

REFERENCES

An, G., Ebert, P.R., Mitra, A., and Ha, S.B. (1988). Binary vectors. In Plant Molecular Biology, S.B. Gelvin and R.A. Schilperoot, eds (Amsterdam: Martinus Nijhoff), pp. 1–19.

Baird, W.V., and Meagher, R.B. (1987). A complex gene superfamily encodes actin in petunia. EMBO J. **6,** 3223–3231.

Carpenter, J.L., Ploense, S., Snustad, D.P., and Silflow, C.D. (1992). Preferential expression of an α-tubulin gene of Arabidopsis in pollen. Plant Cell **4,** 557–571.

Cavener, D.R. (1987). Combinatorial control of structural genes in Drosophila: Solutions that work for the animal. BioEssays **7,** 103–107.

Cleary, A.L., Brown, R.C., and Lemmon, B.E. (1992). Microtubule arrays during mitosis in monoplastidic root tip cells of *Isoetes*. Protoplasma **167,** 123–133.

Cooney, M., Czernuszewicz, G., Postel, E.H., Flint, S.J., and Hogan, M.E. (1988). Site-specific oligonucleotide binding represses transcription of the human c-*myc* gene in vitro. Science **241,** 456–459.

Devereaux, J., Haeberli, P., and Smithies, O. (1984). A comprehensive set of sequence analysis programs for the VAX. Nucleic Acids Res. **12,** 387–395.

Dickinson, W.J. (1988). On the architecture of regulatory systems: Evolutionary insights and implications. BioEssays **8,** 204–208.

Drouin, G., and Dover, G.A. (1990). Independent gene evolution in the potato actin gene family demonstrated by phylogenetic procedures for resolving gene conversions and the phylogeny of angiosperm actin genes. J. Mol. Evol. **31,** 132–150.

Feinberg, A.P., and Vogelstein, B. (1983). A technique for radiolabeling DNA restriction endonuclease fragments to high specific activity. Anal. Biochem. **132,** 6–13 and addendum.

Foley, K.P., and Engel, J.D. (1992). Individual stage selector element mutations lead to reciprocal changes in β- vs ε-globin gene transcription: Genetic confirmation of promoter competition during globin gene switching. Genes Dev. **6,** 730–744.

Frohman, M.A., Dush, M.K., and Martin, G.R. (1988). Rapid production of full-length cDNAs from rare transcripts: Amplification using a single gene-specific oligonucleotide primer. Proc. Natl. Acad. Sci. USA **85,** 8998–9002.

Gilman, M. (1989). Ribonuclease protection assay. In Current Protocols in Molecular Biology, F.M. Ausubel, R. Brent, R.E. Kingston, D.D. Moore, J.G. Seidman, J.A. Smith, and K. Struhl, eds (New York: John Wiley and Son), pp. 4.7.1–4.7.8.

Hemerly, A.S., Ferreira, P., Engler, J.D., Van Montagu, M., Engler, G., and Inzé, D. (1993). *cdc2a* expression in Arabidopsis is linked with competence for cell division. Plant Cell **5,** 1711–1723.

Heslop-Harrison, J., Heslop-Harrison, Y., Cresti, M., Tiezzi, A., and Ciampolini, R. (1986). Actin during pollen germination. J. Cell Sci. **86,** 1–8.

Hightower, R.C., and Meagher, R.B. (1985). Divergence and differential expression of soybean actin genes. EMBO J. **4,** 1–8.

Hightower, R.C., and Meagher, R.B. (1986). The molecular evolution of actin. Genetics **114,** 315–332.

Jefferson, R.A., Kavanagh, T.A., and Bevan, M.W. (1987). GUS fusions: β-Glucuronidase as a sensitive and versatile gene fusion marker in higher plants. EMBO J. **6,** 3901–3907.

Kobayashi, H., Fukuda, H., and Shibaoka, H. (1987). Reorganization of actin filaments associated with the differentiation of tracheary elements in *Zinnia* mesophyll cells. Protoplasma **138,** 69–71.

Kozak, M. (1989). The scanning model for translation: An update. J. Cell Biol. **108,** 229–241.

Lancelle, S.A., Cresti, M., and Hepler, P.K. (1987). Ultrastructure of the cytoskeleton in freeze substituted pollen tubes of *Nicotiana alata*. Protoplasma **140,** 141–150.

Lloyd, C.W., ed (1991). The Cytoskeletal Basis of Plant Growth and Form. (London: Academic Press).

Logemann, J., Schell, J., and Willmitzer, L. (1987). Improved method of isolation of RNA from plant tissues. Anal. Biochem. **163,** 16–20.

Lu, G., and Ferl, R.J. (1992). Site-specific oligodeoxynucleotide binding to maize Adh1 gene promoter represses Adh1-GUS gene expression in vivo. Plant Mol. Biol. **19,** 715–723.

Marton, L., and Browse, J. (1991). Facile transformation of Arabidopsis. Plant Cell Rep. **10,** 235–239.

Mascarenhas, J.P. (1993). Molecular mechanisms of pollen tube growth and differentiation. Plant Cell **5,** 1303–1314.

McCormick, S. (1993). Male gametophyte development. Plant Cell **5,** 1265–1275.

McDowell, J.M., Huang, S., McKinney, E.C., An, Y.-Q., and Meagher, R.B. (1996). Arabidopsis thaliana contains ten actin genes encoding six ancient protein subclasses. Genetics, in press.

McElroy, D., Rothenberg, M., Reece, K.S., and Wu, R. (1990a). Characterization of the rice (*Oryza sativa*) actin gene family. Plant Mol. Biol. **15,** 257–268.

McElroy, D., Zhang, W., Cao, J., and Wu, R. (1990b). Isolation of an efficient actin promotor for use in rice transformation. Plant Cell **2,** 163–171.

McHugh, K.M., Crawford, K., and Lessard, J.L. (1991). A comprehensive analysis of the developmental and tissue-specific expression of the isoactin multigene family in the rat. Dev. Biol. **148,** 442–458.

McKinney, E.C., Ali, N., Traut, A., Feldmann, K.A., Belostotsky, D.A., McDowell, J.A., and Meagher, R.B. (1995). Sequence based identification of T-DNA insertion mutations in Arabidopsis: Actin mutants *act2-1* and *act4-1*. Plant J. **8,** 613–622.

McLean, B.G., Eubanks, S., and Meagher, R.B. (1990). Tissue specific expression of divergent actins in soybean root. Plant Cell **2,** 335–344.

McLean, M., Baird, W.V., Gerats, A.G.M., and Meagher, R.B. (1988). Determination of copy number and linkage relationships among five actin gene subfamilies in *Petunia hybrida*. Plant Mol. Biol. **11,** 663–672.

Meagher, R.B. (1995). The impact of historical contingency on gene phylogeny: Plant actin diversity. In Evolutionary Biology, Vol. 28, M.K. Hecht, R.J. MacIntyre, and M.T. Clegg, eds (New York: Plenum Press), pp. 195–215.

Meagher, R.B., and Williamson, R.E. (1994). The plant cytoskeleton. In Arabidopsis, E. Meyerowitz and C. Somerville, eds (Cold Spring Harbor, NY: Cold Spring Harbor Laboratories), pp. 1049–1084.

Meagher, R.B., Berry-Lowe, S., and Rice, K. (1989). Molecular evolution of the small subunit of ribulose bisphosphate carboxylase: Nucleotide substitution and gene conversion. Genetics **123,** 845–863.

Medford, J.I., Elmer, J.S., and Klee, H.J. (1991). Molecular cloning and characterization of genes expressed in shoot apical meristems. Plant Cell **3,** 359–370.

Meyerowitz, E.M. (1989). Arabidopsis, a useful weed. Cell **56,** 263–269.

Mineyuki, Y., and Gunning, B.E.S. (1990). A role for preprophase bands of microtubules in maturation of new cell walls, and a general proposal on the function of preprophase band sites in cell division in higher plants. J. Cell Sci. **97,** 527–537.

Mueller, P.R., and Wold, B. (1989). In vivo footprinting of a muscle specific enhancer by ligation mediated PCR. Science **246,** 780–786.

Nairn, C.J., Winesett, L., and Ferl, R.J. (1988). Nucleotide sequence of an actin gene from *Arabidopsis thaliana.* Gene **65,** 247–257.

Nakajima-Iijima, S., Hamada, H., Reddy, P., and Kakunaga, T. (1985). Molecular structure of the human cytoplasmic β-actin gene: Interspecies homology of sequences in the introns. Proc. Natl. Acad. Sci. USA **82,** 6133–6137.

Palevitz, B.A. (1987). Actin in the preprophase band of *Allium cepa.* J. Cell Biol. **104,** 1515–1520.

Palevitz, B.A., and Liu, B. (1992). Microfilaments (F-actin) in generative cells and sperm: An evaluation. Sex. Plant Reprod. **5,** 89–100.

Parthasarathy, M.V., Perdue, T.D., Witzmun, A., and Alvernaz, J. (1985). Actin network as a normal component of the cytoskeleton in many vascular plant cells. Am. J. Bot. **72,** 1318–1323.

Pearson, L., and Meagher, R.B. (1990). Diverse soybean actin transcripts contain a large intron in the 5′ untranslated leader: Structural similarity to vertebrate muscle actin genes. Plant Mol. Biol. **14,** 513–526.

Perdue, T.D., and Parthasarathy, M.V. (1985). In situ localization of F-actin in pollen tubes. Eur. J. Cell Biol. **39,** 13–20.

Pierson, E.S., Derksen, J., and Traas, J.A. (1986). Organization of microfilaments and microtubules in pollen tubes grown in vitro or in vivo in various angiosperms. Eur. J. Cell Biol. **41,** 14–18.

Sambrook, J., Fritsch, E.F., and Maniatis, T. (1989). Molecular Cloning: A Laboratory Manual. (Cold Spring Harbor, NY: Cold Spring Harbor Laboratory).

Senecoff, J., and Meagher, R.B. (1993). Isolating the *Arabidopsis thaliana* genes for *de novo* purine synthesis by suppression of *Escherichia coli* mutants: 5′-Phosphoribosyl-5-aminoimadazole synthetase. Plant Physiol. **103,** 387–399.

Shimada, T., Fujii, H., and Lin, H. (1989). A 165-base pair sequence between the dihydrofolate reductase gene and the divergently transcribed upstream gene is sufficent for bidirectional transcriptional activity. J. Biol. Chem. **264,** 20171–20174.

Staiger, C.J., and Schliwa, M. (1987). Actin localization and function in higher plants. Protoplasma **141,** 1–12.

Steer, M.W. (1990). Role of actin in tip growth. In Tip Growth in Plant and Fungal Cells, I.B. Heath, ed (San Diego, CA: Academic Press), pp. 119–145.

Steer, M.W., and Steer, J.M. (1989). Pollen tube tip growth. New Phytol. **111,** 323–358.

Tanzer, M.M., and Meagher, R.B. (1994). Faithful degradation of soybean *rbcS* mRNA *in vitro.* Mol. Cell. Biol. **14,** 2640–2650.

Thangavelu, M., Belostotsky, D., Bevan, M.W., Flavell, R.B., Rogers, H.J., and Lonsdale, D.M. (1993). Partial characterization of the *Nicotiana tabacum* actin gene family: Evidence for pollen specific expression of one of the gene family members. Mol. Gen. Genet. **240,** 290–295.

Thompson, D.M., Tanzer, M.M., and Meagher, R.B. (1992). Degradation products of the mRNA encoding the small subunit of ribulose-1,5-bisphosphate carboxylase in soybean and transgenic petunia. Plant Cell **4,** 47–58.

Tiwari, S.C., and Polito, V.S. (1988). Organization of the cytoskeleton in pollen tubes of *Pyrus communis*: A study employing conventional and freeze substitution electron microscopy, immunofluorescence, and rhodamine-phalloidin. Protoplasma **147,** 100–112.

Twell, D., Yamaguchi, J., and McCormick, S. (1990). Pollen-specifc gene expression in transgenic plants: Coordinate regulation of two different tomato gene promoters during microsporogenesis. Development **109,** 705–713.

White, R.G., and Sack, R.D. (1990). Actin microfilaments in the presumptive statocytes of root caps and coleoptiles. Am. J. Bot. **77,** 17–26.

Wolfe, K.H., Sharp, P.M., and Li, W.-H. (1989). Rates of synonymous substitution in plant nuclear genes. J. Mol. Evol. **29,** 208–211.

Ytow, N., Yamada, T., and Ishizaka, S. (1992). Mechanics of the chloroplast rotation in *Mougeotia*: Measurement of angular velocity by laser diffractometry. Cell Motil. Cytoskeleton **23,** 102–110.

Zhang, W., McElroy, D., and Wu, R. (1991). Analysis of rice *Act1* 5′ region activity in transgenic rice plants. Plant Cell **3,** 1155–1165.